Search for high-energy muon neutrinos from the "naked-eye" GRB080319B with the IceCube neutrino telescope

The IceCube Collaboration

This work was supported by the Director, Office of Science, Office of Basic Energy Sciences, of the U.S. Department of Energy under Contract No. DE-AC02-05CH11231.

Search for high-energy muon neutrinos from the "naked-eye" GRB 080319B with the IceCube neutrino telescope

IceCube Collaboration: R. Abbasi[1], Y. Abdou[2], M. Ackermann[3], J. Adams[4], M. Ahlers[5], K. Andeen[1], J. Auffenberg[6], X. Bai[7], M. Baker[1], S. W. Barwick[8], R. Bay[9], J. L. Bazo Alba[3], K. Beattie[10], S. Bechet[11], J. K. Becker[12], K.-H. Becker[6], M. L. Benabderrahmane[3], J. Berdermann[3], P. Berghaus[1], D. Berley[13], E. Bernardini[3], D. Bertrand[11], D. Z. Besson[14], M. Bissok[15], E. Blaufuss[13], D. J. Boersma[1], C. Bohm[16], J. Bolmont[3], S. Böser[3], O. Botner[17], L. Bradley[18], J. Braun[1], D. Breder[6], T. Burgess[16], T. Castermans[19], D. Chirkin[1], B. Christy[13], J. Clem[7], S. Cohen[20], D. F. Cowen[18,21], M. V. D'Agostino[9], M. Danninger[4], C. T. Day[10], C. De Clercq[22], L. Demirörs[20], O. Depaepe[22], F. Descamps[2], P. Desiati[1], G. de Vries-Uiterweerd[2], T. DeYoung[18], J. C. Diaz-Velez[1], J. Dreyer[12], J. P. Dumm[1], M. R. Duvoort[23], W. R. Edwards[10], R. Ehrlich[13], J. Eisch[1], R. W. Ellsworth[13], O. Engdegård[17], S. Euler[15], P. A. Evenson[7], O. Fadiran[24], A. R. Fazely[25], T. Feusels[2], K. Filimonov[9], C. Finley[1], M. M. Foerster[18], B. D. Fox[18], A. Franckowiak[26], R. Franke[3], T. K. Gaisser[7], J. Gallagher[27], R. Ganugapati[1], L. Gerhardt[10,9], L. Gladstone[1], A. Goldschmidt[10], J. A. Goodman[13], R. Gozzini[28], D. Grant[18], T. Griesel[28], A. Groß[4,29], S. Grullon[1], R. M. Gunasingha[25], M. Gurtner[6], C. Ha[18], A. Hallgren[17], F. Halzen[1], K. Han[4], K. Hanson[1], Y. Hasegawa[30], J. Heise[23], K. Helbing[6], P. Herquet[19], S. Hickford[4], G. C. Hill[1], K. D. Hoffman[13], K. Hoshina[1], D. Hubert[22], W. Huelsnitz[13], J.-P. Hülß[15], P. O. Hulth[16], K. Hultqvist[16], S. Hussain[7], R. L. Imlay[25], M. Inaba[30], A. Ishihara[30], J. Jacobsen[1], G. S. Japaridze[24], H. Johansson[16], J. M. Joseph[10], K.-H. Kampert[6], A. Kappes[1,31], T. Karg[6], A. Karle[1], J. L. Kelley[1], P. Kenny[14], J. Kiryluk[10,9], F. Kislat[3], S. R. Klein[10,9], S. Klepser[3], S. Knops[15], G. Kohnen[19], H. Kolanoski[26], L. Köpke[28], M. Kowalski[26], T. Kowarik[28], M. Krasberg[1], K. Kuehn[32], T. Kuwabara[7], M. Labare[11], K. Laihem[15], H. Landsman[1], R. Lauer[3], H. Leich[3], D. Lennarz[15], A. Lucke[26], J. Lundberg[17], J. Lünemann[28], J. Madsen[33], P. Majumdar[3], R. Maruyama[1], K. Mase[30], H. S. Matis[10], C. P. McParland[10], K. Meagher[13], M. Merck[1], P. Mészáros[21,18], E. Middell[3], N. Milke[12], H. Miyamoto[30], A. Mohr[26], T. Montaruli[1,34], R. Morse[1], S. M. Movit[21], K. Münich[12], R. Nahnhauer[3], J. W. Nam[8], P. Nießen[7], D. R. Nygren[10,16], S. Odrowski[29], A. Olivas[13], M. Olivo[17], M. Ono[30], S. Panknin[26], S. Patton[10], C. Pérez de los Heros[17], J. Petrovic[11], A. Piegsa[28], D. Pieloth[3], A. C. Pohl[17,35], R. Porrata[9], N. Potthoff[6], P. B. Price[9], M. Prikockis[18], G. T. Przybylski[10], K. Rawlins[36], P. Redl[13], E. Resconi[29], W. Rhode[12], M. Ribordy[20], A. Rizzo[22], J. P. Rodrigues[1], P. Roth[13], F. Rothmaier[28], C. Rott[32], C. Roucelle[29], D. Rutledge[18], D. Ryckbosch[2], H.-G. Sander[28], S. Sarkar[5], K. Satalecka[3], S. Schlenstedt[3], T. Schmidt[13], D. Schneider[1], A. Schukraft[15], O. Schulz[29], M. Schunck[15], D. Seckel[7], B. Semburg[6], S. H. Seo[16],

Y. Sestayo[29], S. Seunarine[4], A. Silvestri[8], A. Slipak[18], G. M. Spiczak[33], C. Spiering[3], M. Stamatikos[39], T. Stanev[7], G. Stephens[18], T. Stezelberger[10], R. G. Stokstad[10], M. C. Stoufer[10], S. Stoyanov[7], E. A. Strahler[1], T. Straszheim[13], K.-H. Sulanke[3], G. W. Sullivan[13], Q. Swillens[11], I. Taboada[37], O. Tarasova[3], A. Tepe[6], S. Ter-Antonyan[25], C. Terranova[20], S. Tilav[7], M. Tluczykont[3], P. A. Toale[18], D. Tosi[3], D. Turčan[13], N. van Eijndhoven[23], J. Vandenbroucke[9], A. Van Overloop[2], B. Voigt[3], C. Walck[16], T. Waldenmaier[26], M. Walter[3], C. Wendt[1], S. Westerhoff[1], N. Whitehorn[1], C. H. Wiebusch[15], A. Wiedemann[12], G. Wikström[16], D. R. Williams[38], R. Wischnewski[3], H. Wissing[15,13], K. Woschnagg[9], X. W. Xu[25], G. Yodh[8], and S. Yoshida[30]

Email of corresponding author: kappes@physik.uni-erlangen.de

[1]Dept. of Physics, University of Wisconsin, Madison, WI 53706, USA

[2]Dept. of Subatomic and Radiation Physics, University of Gent, B-9000 Gent, Belgium

[3]DESY, D-15735 Zeuthen, Germany

[4]Dept. of Physics and Astronomy, University of Canterbury, Private Bag 4800, Christchurch, New Zealand

[5]Dept. of Physics, University of Oxford, 1 Keble Road, Oxford OX1 3NP, UK

[6]Dept. of Physics, University of Wuppertal, D-42119 Wuppertal, Germany

[7]Bartol Research Institute and Department of Physics and Astronomy, University of Delaware, Newark, DE 19716, USA

[8]Dept. of Physics and Astronomy, University of California, Irvine, CA 92697, USA

[9]Dept. of Physics, University of California, Berkeley, CA 94720, USA

[10]Lawrence Berkeley National Laboratory, Berkeley, CA 94720, USA

[11]Université Libre de Bruxelles, Science Faculty CP230, B-1050 Brussels, Belgium

[12]Dept. of Physics, TU Dortmund University, D-44221 Dortmund, Germany

[13]Dept. of Physics, University of Maryland, College Park, MD 20742, USA

[14]Dept. of Physics and Astronomy, University of Kansas, Lawrence, KS 66045, USA

[15]III Physikalisches Institut, RWTH Aachen University, D-52056 Aachen, Germany

[16]Dept. of Physics, Stockholm University, SE-10691 Stockholm, Sweden

[17]Dept. of Physics and Astronomy, Uppsala University, Box 516, S-75120 Uppsala, Sweden

[18]Dept. of Physics, Pennsylvania State University, University Park, PA 16802, USA

[19]University of Mons-Hainaut, 7000 Mons, Belgium

[20]Laboratory for High Energy Physics, École Polytechnique Fédérale, CH-1015 Lausanne, Switzerland

[21]Dept. of Astronomy and Astrophysics, Pennsylvania State University, University Park, PA 16802, USA

[22]Vrije Universiteit Brussel, Dienst ELEM, B-1050 Brussels, Belgium

[23]Dept. of Physics and Astronomy, Utrecht University/SRON, NL-3584 CC Utrecht, The Netherlands

[24]CTSPS, Clark-Atlanta University, Atlanta, GA 30314, USA

[25]Dept. of Physics, Southern University, Baton Rouge, LA 70813, USA

[26]Institut für Physik, Humboldt-Universität zu Berlin, D-12489 Berlin, Germany

[27]Dept. of Astronomy, University of Wisconsin, Madison, WI 53706, USA

[28]Institute of Physics, University of Mainz, Staudinger Weg 7, D-55099 Mainz, Germany

[29]Max-Planck-Institut für Kernphysik, D-69177 Heidelberg, Germany

[30]Dept. of Physics, Chiba University, Chiba 263-8522, Japan

ABSTRACT

We report on a search with the IceCube detector for high-energy muon neutrinos from GRB 080319B, one of the brightest gamma-ray bursts (GRBs) ever observed. The fireball model predicts that a mean of 0.12 events should be detected by IceCube for a bulk Lorentz boost of the jet of 300. In both the direct on-time window of 66 s and an extended window of about 300 s around the GRB, there was no excess found above the background. The 90% C.L. upper limit on the number of track-like events from the GRB is 2.7, corresponding to a muon neutrino fluence limit of $9.0 \times 10^{-3}\,\mathrm{erg\,cm^{-2}}$ in the energy range between 145 TeV and 2.1 PeV, which contains 90% of the expected events.

Subject headings: Neutrino telescope, IceCube, cosmic high-energy neutrinos, gamma-ray-burst, GRB 080319B

1. Introduction

Long duration gamma-ray bursts (GRBs) are thought to originate from the collapse of a massive star into a black hole thereby releasing a huge amount of energy in γ-rays into the surrounding medium. Assuming an isotropic emission of these γ-rays the measured fluxes yield an isotropic equivalent energy of $\mathcal{O}(10^{52}$–$10^{53}\,\mathrm{erg})$. However, the actual released

[31]affiliated with Universität Erlangen-Nürnberg, Physikalisches Institut, D-91058, Erlangen, Germany

[32]Dept. of Physics and Center for Cosmology and Astro-Particle Physics, The Ohio State University, 191 W. Woodruff Ave., Columbus, OH 43210, USA

[33]Dept. of Physics, University of Wisconsin, River Falls, WI 54022, USA

[34]on leave of absence from Università di Bari and Sezione INFN, Dipartimento di Fisica, I-70126, Bari, Italy

[35]affiliated with School of Pure and Applied Natural Sciences, Kalmar University, S-39182 Kalmar, Sweden

[36]Dept. of Physics and Astronomy, University of Alaska Anchorage, 3211 Providence Dr., Anchorage, AK 99508, USA

[37]School of Physics and Center for Relativistic Astrophysics, Georgia Institute of Technology, Atlanta, GA 30332. USA

[38]Dept. of Physics and Astronomy, University of Alabama, Tuscaloosa, AL 35487, USA

[39]Astroparticle Physics Laboratory, Code 661, NASA/Goddard Space Flight Center, Greenbelt, MD 20771, USA

energy can be significantly lower if the γ-rays are only emitted within a small cone (jet) as suggested by the observation of signatures for jet breaks in some X-ray spectra. Apart from being one of the most violent events in the universe GRBs are also one of the few plausible source candidates for ultra-high energy cosmic rays. Though our knowledge about GRBs has greatly increased in recent years, their exact nature, the way in which particles are accelerated, and the composition and generation of the jets formed from material accreted onto the black hole are still not fully understood.

The observation of high-energy neutrinos from GRBs would be a smoking gun for the acceleration of hadrons in the jets and hence for the connection between GRBs and extra-Galactic cosmic rays. In the fireball model (Meszaros & Rees 1993) the interaction of accelerated protons with synchrotron photons radiated by accelerated electrons leads to the production of pions (Waxman & Bahcall 1997). In the leptonic decay of the charged pions high-energy neutrinos are produced with the ratios $(\nu_e{:}\nu_\mu{:}\nu_\tau) = (1{:}2{:}0)$ [1], changing to (1:1:1) at Earth due to oscillations[2]. The acceleration of both electrons and protons is thought to occur in internal shock fronts caused by colliding shells emitted from the accretion region around the black hole. The distance of the collision region from the black hole is determined to a large extent by the bulk Lorentz boost of the jet, $\Gamma_{\rm jet}$, and increases as $\Gamma^2_{\rm jet}$. The first calculations of the expected neutrino flux from GRBs (Waxman & Bahcall 1997; Alvarez-Muniz & Halzen 1999) used average GRB parameters and the GRB rate measured by BATSE to determine an all-sky neutrino flux from the GRB population. This so called Waxman-Bahcall GRB flux or similar GRB fluxes have been probed with the AMANDA-II neutrino telescope (Achterberg et al. 2007, 2008) with negative results so far. These fluxes will be detectable by next-generation neutrino telescopes like IceCube with an instrumented volume of $\geq 1\,\mathrm{km}^3$. However, the derived average flux for a single burst in these models is very small even for $1\,\mathrm{km}^3$ detectors. Nevertheless, as the expected neutrino flux can actually vary by orders of magnitude between GRBs due to fluctuations in the model parameters (Alvarez-Muniz et al. 2000; Becker et al. 2006) the detection of extremely bright GRBs in neutrinos does seem possible. However, the detection of these bright GRBs requires at least a km^3-size detector, as for example was demonstrated in the analysis of GRB 030329 with the AMANDA detector (Stamatikos et al. 2005).

On March 19, 2008, at 06:12:49 UT GRB 080319B (Racusin et al. 2008a) was detected by the Swift (Burrows et al. 2005) and Konus-Wind (NASA 1994) satellites. It was the

[1]Here and throughout the rest of the paper ν denotes both neutrinos and anti-neutrinos.

[2]Kashti & Waxman (2005) showed that above a certain energy (typically $\mathcal{O}(10\,\mathrm{PeV})$) the ratio changes to (1:1.8:1.8) due to cooling energy losses of the muons producing the neutrinos.

optically brightest GRB ever observed and with a peak magnitude of 5.3 even visible to the naked eye for a short period of time, despite the fact that the corresponding redshift was about 0.9. It is also one of best measured GRBs with optical wide-field observations covering the whole duration of the explosion (Cwiok et al. 2008) and with many triggered follow-up observations spanning the electromagnetic energy spectrum from radio to γ-rays (Racusin et al. 2008a).

2. Neutrino spectrum calculation

We calculate the expected prompt neutrino spectrum for GRB 080319B using the model from Waxman & Bahcall (1997). This model allows for the easy incorporation of many measured parameters of GRB 080319B (in the paper itself average GRB parameters are used) which is crucial when investigating a GRB that deviates largely from the average GRB. Other models like Murase & Nagataki (2006)[3] or Razzaque et al. (2003) do not provide this possibility and are therefore not considered here.

The calculation of the expected neutrino spectrum requires a knowledge of the γ-ray spectrum. It is derived from the published fits to the Swift and Konus-Wind data (Racusin et al. 2008b; Golenetskii et al. 2008), and is displayed in Fig. 1a. Due to its limited energy range of 15–350 keV the break in the energy spectrum was not observed by the Swift BAT instrument. Konus-Wind with its energy band of 25 keV–7 MeV fitted a Band function (Band et al. 1993) to its data. In our calculations, we adopt a broken power-law parameterization with spectral indices equal to those measured by Konus-Wind and adjust the break energy in such a way that the resulting integrated fluence agrees with those measured by Swift and Konus-Wind in their respective energy ranges. The parameters of the γ-ray spectrum are listed in Table 1.

The neutrino spectrum also requires the knowledge of further parameters listed in Table 1. Not all of of these are measured or even well known. For the jet parameters f_e (fraction of jet energy in electrons) and f_b (fraction of jet energy in baryons) typical values of 0.1 were used (Becker 2008). The variability of the γ-ray flux $t_{\rm var}$, which is used as a measure for the time between the emission of two consecutive shells, was analyzed in Margutti et al. (2008). They find an initial time-scale of 0.1 s which increased to 0.7 s in the course of the emission. However, their analysis was limited to the energy range between 15 and 150 keV, where for

[3]This model is actually similar to Waxman & Bahcall (1997) but uses Monte Carlo simulation to calculate the photomeson production in $p\gamma$ interactions and takes the synchrotron losses of mesons and protons into account.

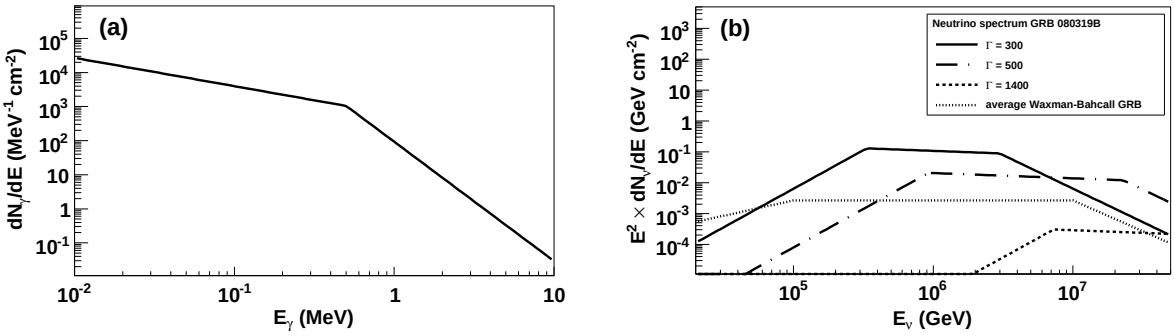

Fig. 1.— (a) γ-ray spectrum according to the Swift and Konus-Wind observations. (b) Calculated muon neutrino spectrum for different bulk Lorentz boosts $\Gamma_{\rm jet}$ of the GRB jet. Also shown is the average Waxman-Bahcall GRB flux.

high energies (100–150 keV) the dominant time-scale was significantly shorter (0.05 s). By contrast, muons reconstructed in the IceCube detector are mainly produced by neutrinos near the first break energy (Fig. 1b and 5b) which originate from proton interactions with γ-rays around 500 keV (break energy in γ-ray spectrum). Due to the large gap between 150 and 500 keV and the lack of an extrapolation method we used a typical value of $t_{\rm var} = 0.01\,{\rm s}$ (Becker 2008) in our calculations.

For reference we list here the formulae used:

$$F_\gamma(E_\gamma) = f_\gamma \times \begin{cases} \epsilon_\gamma^{\alpha_\gamma-\beta_\gamma}\ E_\gamma^{-\alpha_\gamma} & \text{for } E_\gamma < \epsilon_\gamma \\ E_\gamma^{-\beta_\gamma} & \text{for } E_\gamma \geq \epsilon_\gamma \end{cases} \tag{1}$$

$$\mathcal{F}_\gamma = \int_{20\,{\rm keV}}^{7\,{\rm MeV}} {\rm d}E_\gamma\ F_\gamma(E_\gamma) \tag{2}$$

$$F_\nu(E_\nu) = f_\nu \times \begin{cases} \epsilon_1^{\alpha_\nu-\beta_\nu}\ E_\nu^{-\alpha_\nu} & \text{for } E_\nu < \epsilon_1 \\ E_\nu^{-\beta_\nu} & \text{for } \epsilon_1 \leq E_\nu < \epsilon_2 \\ \epsilon_2^{\gamma_\nu-\beta_\nu}\ E_\nu^{-\gamma_\nu} & \text{for } E_\nu \geq \epsilon_2 \end{cases} \tag{3}$$

$$\epsilon_1 = 7.5\times10^5\,{\rm GeV}\ \frac{1}{(1+z)^2}\left(\frac{\Gamma_{\rm jet}}{10^{2.5}}\right)^2\left(\frac{\rm MeV}{\epsilon_\gamma}\right) \tag{4}$$

$$\epsilon_2 = 10^7\,{\rm GeV}\ \frac{1}{1+z}\ \sqrt{\frac{f_e}{f_b}}\ \left(\frac{\Gamma_{\rm jet}}{10^{2.5}}\right)^4\left(\frac{t_{\rm var}}{0.01\,{\rm s}}\right)\ \sqrt{\frac{10^{52}\,{\rm erg\,s^{-1}}}{L_\gamma^{\rm iso}}} \tag{5}$$

$$\alpha_\nu = 3 - \beta_\gamma \quad , \quad \beta_\nu \; = \; 3 - \alpha_\gamma \quad , \quad \gamma_\nu = \beta_\nu + 2 \tag{6}$$

$$\frac{\Delta R}{\lambda_{p\gamma}} = \left(\frac{L_\gamma^{\rm iso}}{10^{52}\,{\rm erg\,s^{-1}}}\right)\,\left(\frac{0.01\,{\rm s}}{t_{\rm var}}\right)\,\left(\frac{10^{2.5}}{\Gamma_{\rm jet}}\right)^4\,\left(\frac{\rm MeV}{\epsilon_\gamma}\right) \tag{7}$$

$$\int_0^\infty {\rm d}E_\nu\; F_\nu(E_\nu) = \frac{1}{8}\,\frac{1}{f_e}\,\left(1-(1-\langle x_{p\to\pi}\rangle)^{\Delta R/\lambda_{p\gamma}}\right)\int_0^\infty {\rm d}E_\gamma\; F_\gamma(E_\gamma) \tag{8}$$

where ϵ_γ is the photon spectrum break energy, and α_γ and β_γ are the spectrum indices before and after the break energy, respectively. The quantity $\mathcal{F}_\gamma = 6.23 \times 10^{-4}\,{\rm erg\,cm^{-2}}$ is the measured γ-ray fluence (Racusin et al. 2008a) and z the redshift of the GRB. The parameters of the neutrino spectrum $F_\nu(E_\nu)$ are the two break energies, ϵ_1 and ϵ_2, and the corresponding spectral indices α_ν, β_ν and γ_ν. The expression $1-(1-\langle x_{p\to\pi}\rangle)^{\Delta R/\lambda_{p\gamma}}$ in equation (8) estimates the overall fraction of the proton energy going into pions from the size of the shock, ΔR, and the mean free path of a proton for photomeson interactions, $\lambda_{p\gamma}$. Here, $\langle x_{p\to\pi}\rangle = 0.2$ is the average fraction of proton energy transferred to a pion in a single interaction. The expression ensures that the transferred energy fraction is ≤ 1. The variables f_γ and f_ν are defined by the integrals of equations (2) and (8). The isotropic equivalent luminosity, $L_\gamma^{\rm iso}$, is given by the isotropic equivalent energy released in γ-rays, $E_\gamma^{\rm iso}$, divided by the burst duration. The calculations are insensitive to the beaming effect caused by a narrow opening angle of the jet (0.4° for GRB 080319B according to Racusin et al. (2008a)) as all formulae contain the isotropic luminosity in conjunction with a 4π shell geometry, i.e. effectively use luminosity per steradian. For example, the target photon density used to calculate $N_{\rm int}$ is given by $n_\gamma \propto L_\gamma^{\rm iso}/4\pi R^2$.

The $\Gamma_{\rm jet}$ factor, which enters the equations above to the second and fourth power, has a large impact on the normalization of the neutrino flux (with increasing distance from the black hole the synchrotron photon field and hence the target density for the pion production decreases). Following the calculations in Guetta et al. (2004) with the parameters given in Table 1 yields a $\Gamma_{\rm jet}$ factor of about 300. In Racusin et al. (2008a) the authors determine the $\Gamma_{\rm jet}$ factor to lie between 300 and 1400. Kumar & Panaitescu (2008) quote a $\Gamma_{\rm jet}$ factor of ~ 500. For the calculation of the neutrino spectrum we adopt the optimistic case with $\Gamma_{\rm jet} = 300$ which is displayed in Fig. 1b as the solid line. An increase of the $\Gamma_{\rm jet}$ factor to 500 (1400) decreases the neutrino flux by about a factor 10 (10^4) and a shift to higher energies (Fig. 1b dashed and dotted lines). Muon cooling (Kashti & Waxman 2005) affects the neutrino spectrum ($\Gamma_{\rm jet} = 300$) only at energies above $\sim 20\,{\rm PeV}$ and is therefore negligible for our analysis.

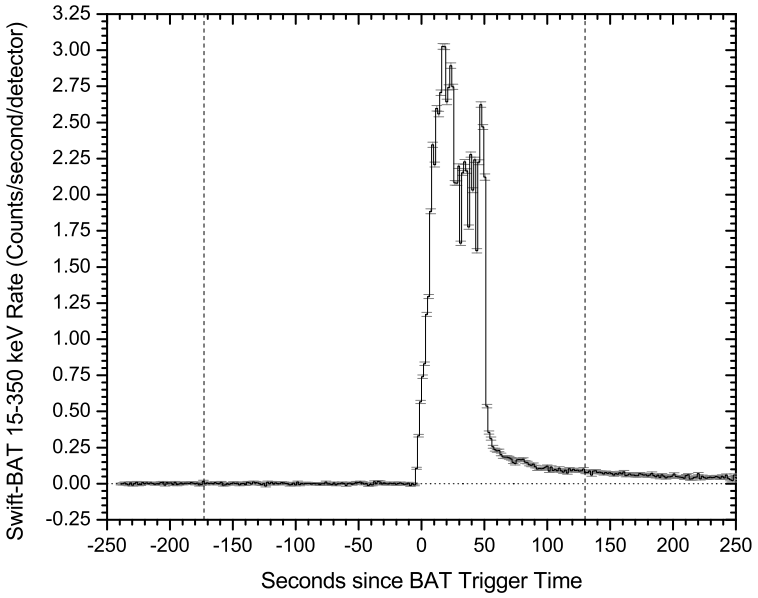

Fig. 2.— γ-ray emission from GRB 080319B as measured by Swift-BAT (Stamatikos 2008) with T_0 = 06:12:49 UT. The dashed vertical lines mark the time range covered by IceCube data.

3. Analysis of IceCube data

IceCube (Achterberg et al. 2006), the successor of the AMANDA experiment and the first next-generation neutrino telescope, is currently being installed in the deep ice at the geographic South Pole. Its final configuration will instrument a volume of about 1 km^3 of clear ice in depths between 1450 m and 2450 m. Neutrinos are reconstructed by detecting the Cherenkov light from charged secondary particles, which are produced in interactions of the neutrinos with the nuclei in the ice or bedrock. The optical sensors consist of photomultipliers housed in pressure-resistant glass spheres (digital optical modules, DOMs, Abbasi et al. (2008)) which are mounted on vertical strings. Each string consists of 60 DOMs with the final detector containing 80 such strings. Physics data taking with IceCube started in 2006 with 9 strings installed. At the beginning of 2007 the detector was enlarged to 22 strings. Since April 2008 IceCube has been running with 40 strings. The completion of the detector construction is planned for the year 2011.

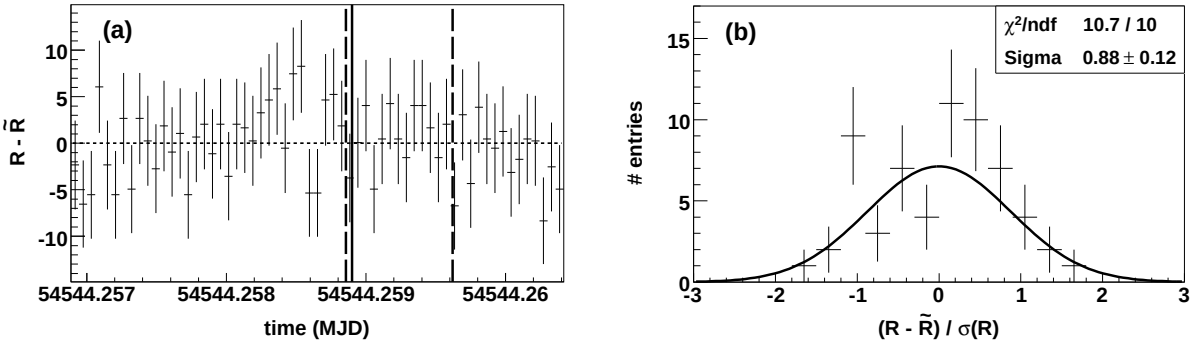

Fig. 3.— (a) Difference between the rate R in a 5 s bin and the average rate $\tilde{R}$ (calculated from all events in the 300 s time window shown) as a function of time. The solid and dashed vertical lines mark the satellite trigger time of the GRB and the start and stop times of the measured γ-ray emission, respectively. (b) Histogram of $(R - \tilde{R})$ divided by the statistical errors. The line is a fit of a Gaussian distribution to the histogram.

3.1. Data sets and reconstruction

The data acquisition (DAQ) system of IceCube (Abbasi et al. 2008) is based on local coincidences between neighboring DOMs for which the photon signal passes a threshold of 0.25 photo-electrons. All data from DOMs belonging to a local coincidence are read out and the digitized waveforms are sent to a computer farm at the surface. In order to pass the trigger a minimum number of 8 DOMs in local coincidences within a time window of 5000 ns is required. If this condition is fulfilled the waveforms are combined to an event and the number and arrival times of the Cherenkov photons are extracted.

At the time of GRB 080319B, IceCube was running in maintenance mode with 9 out of 22 strings taking data. Apart from the reduced number of strings the DAQ system had a slightly different configuration than during normal operation. IceCube data is available in a window of about 300 s around the GRB (on-time data) as displayed in Fig. 2. The detector was checked for stability during this period by plotting the data rate, R, in bins of time relative to the average rate $\tilde{R}$ (pull plot, Fig. 3). The variations in the data rate are compatible with pure statistical fluctuations and there were no indications for abnormal behavior of the detector during the period under consideration.

In order to avoid systematic uncertainties due to inaccuracies in the simulation when calculating the significance of a deviation from the background-only hypothesis, the expected background in the on-time window is determined from the observed off-time data. The low number of signal events expected from the GRB entails that the expected background for the on-time window (after cuts) is $\ll 1$. Such a prediction requires a large off-time background

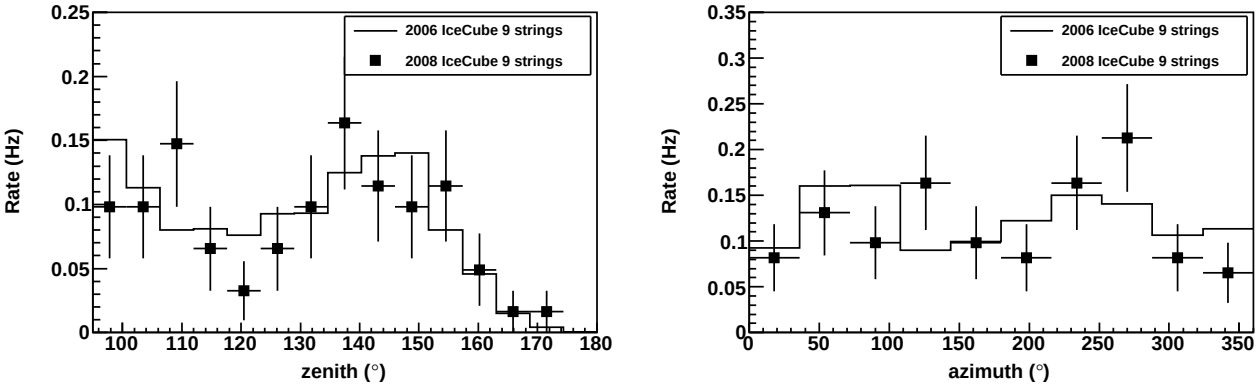

Fig. 4.— Comparison after quality cuts of the background data set (2006 IceCube 9 strings) with a 1 hour data set taken 1 week after GRB 080319B with equivalent DAQ settings (2008 IceCube 9 strings).

data set. The available amount of data taken with the special DAQ configuration during the regular maintenance runs is therefore not sufficient for this analysis. Instead, the IceCube data set of the 2006 data taking period (131 days livetime) is used, when the detector consisted only of the 9 strings which were also taking data during GRB 080319B. Quality cuts (see section 3.2) on reconstructed quantities ensure that the 2006 data set is in very good agreement with the GRB 080319B maintenance data set. Figure 4 shows as examples the comparisons for the zenith and azimuth distributions. The difference in the overall rates is about 10% which is within the statistical error of the total number of events in the maintenance data set.

The direction of a neutrino candidate is determined by fitting a muon-track hypothesis to the pattern of the recorded Cherenkov light in the detector using a log-likelihood reconstruction method (Ahrens et al. 2004). A fit of a paraboloid to the minimum in the log-likelihood space yields an estimate of the uncertainty on the reconstructed direction. After final cuts (see section 3.2) and for neutrinos from the direction of the GRB (weighted according to the calculated GRB spectrum), 90% of all reconstructed Monte Carlo tracks are contained within 20° of the true direction. The median angular resolution is 5.3°. This resolution is worse than the one usually quoted for IceCube in its 9-string configuration for neutrino-induced muons. The reason for this is that the geometry of the detector was such that the reconstruction lever arm was at its shortest for the direction of GRB 080319B. The absolute time of an event is determined with a GPS clock with a precision of better than a ms, which is more than sufficient for this analysis.

3.2. Analysis method

The data around GRB 080319B were analyzed using an unbinned log-likelihood method similar to the one described in Braun et al. (2008). The signal, $S(\vec{x}_i)$, and background, $B(\vec{x}_i)$, probability density functions (PDFs) are each the product of a time PDF and a spatial PDF, where $\vec{x}_i$ denotes both the spatial and time variables. The spatial signal PDF is a two-dimensional Gaussian distribution with the two widths being the major and minor axis of the 1σ error ellipse of the paraboloid fit described in the previous section. The time PDF is flat over the γ-ray emission time and falls off on both sides with a Gaussian distribution with $\sigma = 25\,\mathrm{s}$. The Gaussian accounts for possible small shifts in the neutrino emission time with respect to that of the γ-rays and prevents discontinuities in the likelihood function. The sensitivity of the analysis depends only weakly on the exact choice of σ, e.g. the quoted upper limit changes by less than 2% when doubling σ. For the spatial background PDF the detector asymmetries in zenith and azimuth have to be taken into account. This is accomplished by evaluating the data in the detector coordinate system. The spatial background PDF is hence the probability distribution of all background events after cuts in the zenith-azimuth plane of the detector. The time distribution of background tracks during the GRB can be assumed to be constant resulting in a flat time PDF.

Both PDFs are combined in an extended log-likelihood function (Barlow 1989)

$$\ln\left(\mathcal{L}(\langle n_s\rangle)\right) = -\langle n_s\rangle - \langle n_b\rangle + \sum_{i=1}^{N} \ln\left(\langle n_s\rangle\, S(\vec{x}_i) + \langle n_b\rangle\, B(\vec{x}_i)\right) \ , \tag{9}$$

where the sum runs over all reconstructed tracks left after cuts with $\vec{x}_i$ representing the PDF parameters (absolute time of the track along with the track direction in local detector coordinates and its estimated uncertainty). The variable $\langle n_b\rangle$ is the expected mean number of background events, which is determined from the background data set. The mean number of signal events, $\langle n_s\rangle$, is a free parameter which is varied to maximize the expression

$$\ln\left(\mathcal{R}(\langle n_s\rangle)\right) = \ln\left(\frac{\mathcal{L}(\langle n_s\rangle)}{\mathcal{L}(0)}\right) = -\langle n_s\rangle + \sum_{i=1}^{N} \ln\left(\frac{\langle n_s\rangle\, S_i(\vec{x}_i)}{\langle n_b\rangle\, B_i(\vec{x}_i)} + 1\right) \tag{10}$$

in order to obtain the best estimate for the number of signal events, $\langle \hat{n}_s\rangle$, in the on-time data set.

GRBs are expected to generate a substantially harder neutrino energy spectrum than that of atmospheric neutrinos. A detector quantity closely related to the neutrino energy is the number of DOMs (channels) with detected photons, N_{ch}. This quantity is used to enhance the sensitivity to a possible signal. The N_{ch} background PDF is determined from

all background events left after cuts in the off-time data set which are reconstructed within 20 degrees of the GRB. For a given data set with $\langle \hat{n}_s \rangle > 0$ the track with the highest likelihood contribution is selected and the corresponding probability to observe this or a higher N_{ch} value with respect to the N_{ch} background PDF is calculated. This probability is then multiplied with the p-value from the likelihood distribution. The product is used as the test statistic $\mathcal{T}$ to calculate the final significance. To determine whether a given data set is compatible with the background-only hypothesis a large number of background data sets were generated from the 2006 9-string data by randomizing the track times while taking into account the uptime of the detector. Afterwards, the $\mathcal{T}$ value for each of these data sets was calculated. The p-value for the on-time data set is then given by the fraction of background-only data sets with an equal or larger $\mathcal{T}$ value.

In order to avoid biasing the results the on-time data were kept blind while optimizing the analysis. In a first step, loose cuts were applied on the following reconstructed quantities to improve the signal to background ratio and reduce the amount of data for the likelihood method:

- the uncertainty of the reconstructed track direction, σ_{dir} (quadratic average of the minor and major axis of the 1σ error ellipse),
- the reduced likelihood value of the reconstructed track,
- the number of photons detected within a -15–75 ns time window with respect to the expected arrival time for unscattered photons from the muon track hypothesis, N_{dir} (direct hits),
- the minimum zenith angle from a fit of a two-track hypothesis to the light pattern.

The latter rejects events where two down-going muons from independent atmospheric showers pass through the detector in quick succession and produce a light pattern that fakes an up-going track.

The sensitivity to neutrinos from GRB 080319B was determined by injecting Monte Carlo signal events weighted according to the flux calculated in section 2 ($\Gamma_{\mathrm{jet}} = 300$) and with their true direction equal to that of the GRB. The Monte Carlo contains a detailed simulation of the propagation of the muon neutrino through the Earth and the ice. After the interaction the muon is traced through rock and ice taking into account continuous and stochastic energy losses. The photon signal in the DOMs is determined from a detailed simulation (Lundberg et al. 2007) of the propagation of Cherenkov light through the ice which includes the modeling of the changes in absorption and scattering length with depth (dust layers) (Ackermann et al. 2006). This is followed by a simulation of the DOM electronics and the trigger. The DOM signals are then processed in the same way as the real data.

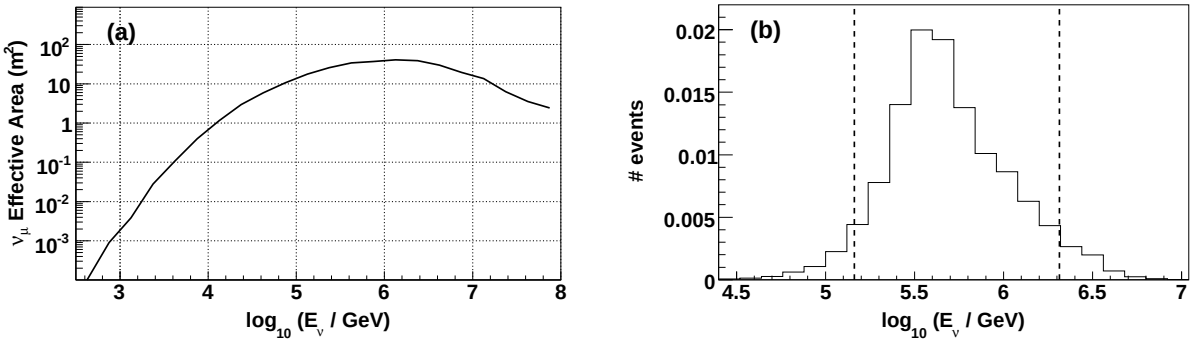

Fig. 5.— (a) Effective area for muon neutrinos from the direction of GRB 080319B as a function of the neutrino energy. (b) Expected mean number of Monte Carlo signal events after final cuts as a function of neutrino energy. The two vertical lines mark the central interval containing 90% of the events.

In order to optimize the chances for discovery (Hill et al. 2005) for the spectrum shape calculated in section 2 ($\Gamma_{\rm jet} = 300$), the cuts on $\sigma_{\rm dir}$ and $N_{\rm dir}$ were tightened until a minimum in the amount of flux required for a 50% chance of a 4σ signal in the detector was reached. The corresponding effective area for muon neutrinos from the direction of the GRB as a function of energy is displayed in Fig. 5a. The optimized cut parameters were then applied to background and the on-time data set, and the likelihood function of the on-time data set was evaluated with respect to the randomized background data sets. The expected mean number of events from the GRB ($\Gamma_{\rm jet} = 300$) after final cuts is 0.12, with 90% of the events contained in the energy range from 145 TeV to 2.1 PeV (Fig. 5b). In this case, the potential for a discovery with a p-value of 6.33×10^{-5} (4σ) or smaller is about 7%.

3.3. Results

After unblinding the on-time data for GRB 080319B, the data were analyzed with respect to two time windows[4]. The shorter one (from $T_0 - 3.8\,\mathrm{s}$ to $T_0 + 62.2\,\mathrm{s}$) corresponds to the immediate emission time of the γ-rays, whereas the second (from $T_0 - 173\,\mathrm{s}$ to $T_0 + 130\,\mathrm{s}$) covers the whole time range with IceCube data (see Fig. 2). No significant deviation from the background-only hypothesis was found in either of the two time windows. In both cases the unbinned likelihood method yields $\langle \hat{n}_s \rangle = 0$ as the best estimate for the number of signal events. Subsequent inspection of all reconstructed tracks in the on-time window at a lower cut level revealed no good neutrino candidate within 10° of the GRB position. The resulting

[4]The time windows define the flat part of the signal time PDFs.

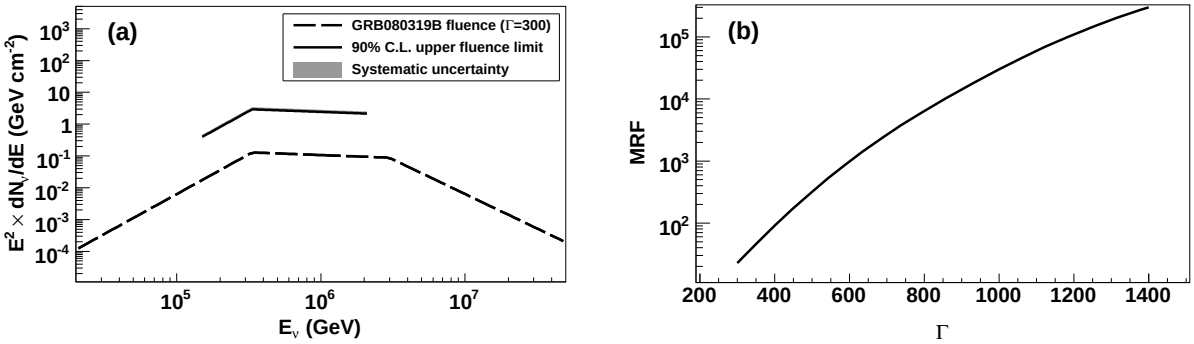

Fig. 6.— (a) 90% C.L. upper limit on the fluence from GRB 080319B with respect to the calculated neutrino fluence for a bulk Lorentz boost of the jet of $\Gamma_{\rm jet} = 300$. The gray area represents the systematic uncertainty on the limit (covered by line of the upper limit). (b) Model rejection factor, MRF, as a function of $\Gamma_{\rm jet}$.

Neyman 90% C.L. upper limit (Amsler et al. 2008) on the number of signal events for the short time window is 2.7. From the neutrino flux calculated in section 2 for $\Gamma_{\rm jet} = 300$ we expect to see 0.12 events. This results in a model rejection factor (MRF) of 22.7 by which the limit has to be scaled down to reach this flux. The resulting upper limit on the muon neutrino fluence is plotted in Fig. 6a in the energy range containing 90% of the detected signal events. Integrating the fluence over this energy range yields an upper limit of $9.0 \times 10^{-3}\,\mathrm{erg\,cm^{-2}}$. This upper limit is slightly conservative as we do not consider the effect of ν_τ from GRBs. Tau neutrinos might manifest themselves as τ tracks (which can travel a substantial distance at PeV energies) or as muons from tau decays[5]. The impact of a larger bulk Lorentz boost on the MRF is displayed in Fig. 6b. In addition, the MRFs for $\Gamma_{\rm jet} = 500$ and 1400 are listed in Table 2.

The effects of systematic errors on the result, described below in detail, were investigated by varying simulation parameters and repeating the full analysis. The quadratic sum of all systematic errors (+17%,−4%) is displayed in Fig. 6a as a gray band (covered by line of upper limit). The main sources of systematic uncertainty are:

Ice simulation: Inaccuracies in the ice simulation can lead to a wrong estimate of the efficiency of the detector to neutrinos from the GRB. In order to estimate the size of this effect the analysis was repeated using a modified ice simulation. In this simulation the DOM efficiency was altered as a function of depth according to the differences observed between data and Monte Carlo in the DOM occupancy, effectively making the ice clearer for depths

[5]Electron neutrinos do not contribute to the signal as the resulting electron immediately produces an electromagnetic cascade.

Table 1. Fireball model parameters used in the calculation of the neutrino spectrum for GRB 080319B

Parameter	Value	Reference
$E_\gamma^{\rm iso}$	$1.3 \times 10^{54}\,{\rm erg\,s^{-1}}$	Racusin et al. (2008a)
Burst duration	66 s	Racusin et al. (2008b)
$\Gamma_{\rm jet}$	300, 500, 1400	Racusin et al. (2008a); see also main text
γ spec.—fluence, $\mathcal{F}_\gamma$ (20 keV–7 MeV)	$6.23 \times 10^{-4}\,{\rm erg\,cm^{-2}}$	Racusin et al. (2008a)
γ spec.—break energy, ϵ_γ	520 keV	see main text
γ spec.—1st index, α_γ	-0.83	Racusin et al. (2008a) (suppl. information)
γ spec.—2nd index, β_γ	-3.5	Racusin et al. (2008a) (suppl. information)
z	0.94	Vreeswijk et al. (2008)
x_π [a]	0.2	Becker (2008)
f_e	0.1	Becker (2008)
f_b	0.1	Becker (2008)
$t_{\rm var}$	0.01 s	Becker (2008)

[a]Fraction of proton energy going into pion in a single $p\gamma$ interaction

Table 2. Neutrino spectrum parameters according to the fireball model for GRB 080319B for different bulk Lorentz factors of the jet together with the expected mean number of events in the detector and the model rejection factor obtained from the analysis

Parameter \ bulk Lorentz factor	$\Gamma_{\rm jet} = 300$	$\Gamma_{\rm jet} = 500$	$\Gamma_{\rm jet} = 1400$
1st break energy, ϵ_1	334 TeV	928 TeV	7.27 PeV
2nd break energy, ϵ_2	2.98 PeV	23.0 PeV	1.41 EeV
1st index, α_ν	0.5	0.5	0.5
2nd index, β_ν	-2.17	-2.17	-2.17
3rd index, γ_ν	-4.17	-4.17	-4.17
Energy fluence at 1st break energy	$0.129\,{\rm GeV\,cm^{-2}}$	$0.021\,{\rm GeV\,cm^{-2}}$	$3.04 \times 10^{-4}\,{\rm GeV\,cm^{-2}}$
Expected events in IceCube	0.12	8.6×10^{-3}	9.6×10^{-6}
MRF	22.7	318	3×10^5

with above-average transparencies and dirtier for depths with below-average transparencies. This leads to an increase of the fluence upper limit of 16%, which is included as a one-sided systematic error;

DOM efficiency: Uncertainties in the efficiency of the optical modules in the photon detection leads to an uncertainty in the number of expected events from the GRB. Varying the efficiency by ±10% changes the upper limit by ±4%;

Background rate: Even after optimized cuts the data set is dominated by mis-reconstructed down-going atmospheric muons. The rate varies throughout the year due to changes in the density profile of the atmosphere at high altitude above the South Pole by about 10% around the mean value. As the number of events after cuts in the data set during the GRB is too low, the rate at the time of the GRB was determined using a 1 hour data set recorded with the same DAQ settings about a week later. In order to account for potential differences the background data rate was varied by ±10%. This results in a shift of the upper limit of less than ±1%.

4. Conclusions and outlook

We used the IceCube neutrino telescope to search for high-energy muon neutrinos from GRB 080319B, one of the most spectacular and well measured GRBs ever observed. Based on the fireball model of GRBs and the measured γ-ray fluence we calculated the expected neutrino spectrum for different jet bulk Lorentz boosts $\Gamma_{\rm jet}$. After applying quality cuts to suppress mis-reconstructed atmospheric muons a mean number of 0.12 signal events is expected for the optimistic case of $\Gamma_{\rm jet} = 300$ (for other $\Gamma_{\rm jet}$ see Table 2) in IceCube, which was running in a 9 string configuration. The data were analyzed with an unbinned log-likelihood method utilizing the spatial and temporal distance of reconstructed tracks to the GRB. Afterwards, the resulting p-value was combined with energy information to enhance the significance of a potential GRB signal. No deviation from the background-only hypothesis was found either in a small time window covering the immediate γ-ray emission time or an extended window of 300 s. This results in a 90% C.L. upper limit on the muon neutrino fluence from GRB 080319B within the short time window of $9.0 \times 10^{-3}\,\mathrm{erg\,cm^{-2}}$ in the energy range between 145 TeV and 2.1 PeV which contains 90% of the expected signal events. The corresponding MRF value for the calculated GRB spectrum is 22.7 with a systematic uncertainty of (+17%,−4%). This upper limit does not allow us to impose constraints on GRB parameters within the fireball model.

In its final configuration with 80 strings the expected number of detected events in

IceCube from a bright GRB like GRB 080319B is $\mathcal{O}(1)$, rendering the individual analysis of these rare GRBs highly interesting also in the future. Using the large number of GRBs observed by the Swift and Fermi (formerly GLAST) satellites, the growing IceCube detector will also soon be able to probe the Waxman-Bahcall or similar GRB fluxes and in the case of a non-detection set stringent limits.

We acknowledge the support from the following agencies: U.S. National Science Foundation-Office of Polar Program, U.S. National Science Foundation-Physics Division, University of Wisconsin Alumni Research Foundation, U.S. Department of Energy, and National Energy Research Scientific Computing Center, the Louisiana Optical Network Initiative (LONI) grid computing resources; Swedish Research Council, Swedish Polar Research Secretariat, and Knut and Alice Wallenberg Foundation, Sweden; German Ministry for Education and Research (BMBF), Deutsche Forschungsgemeinschaft (DFG), Germany; Fund for Scientific Research (FNRS-FWO), Flanders Institute to encourage scientific and technological research in industry (IWT), Belgian Federal Science Policy Office (Belspo); the Netherlands Organisation for Scientific Research (NWO); M. Ribordy acknowledges the support of the SNF (Switzerland); A. Kappes and A. Groß acknowledge support by the EU Marie Curie OIF Program; M. Stamatikos is supported by an NPP Fellowship at NASA-GSFC administered by ORAU.

REFERENCES

Abbasi, R., (IceCube Coll.), et al. 2008, arXiv:0810.4930

Achterberg, A., (IceCube Coll.), et al. 2006, Astropart. Phys., 26, 155

—. 2007, ApJ, 664, 397

—. 2008, ApJ, 674, 357

Ackermann, M., (AMANDA Coll.), et al. 2006, J. Geophys. Res., 111, D13203

Ahrens, J., (AMANDA Coll.), et al. 2004, Nucl. Inst. Meth., A524, 169

Alvarez-Muniz, J., & Halzen, F. 1999, ApJ, 521, 928

Alvarez-Muniz, J., Halzen, F., & Hooper, D. W. 2000, Phys. Rev., D62, 093015

Amsler, C., et al. 2008, Phys. Lett., B667, 1

Band, D., et al. 1993, ApJ, 413, 281

Barlow, R. J. 1989, Statistics (Wiley)

Becker, J. K. 2008, Phys. Rep., 458, 173

Becker, J. K., Stamatikos, M., Halzen, F., & Rhode, W. 2006, Astropart. Phys., 25, 118

Braun, J., Dumm, J., de Palma, F., Finley, C., Karle, A., & Montaruli, T. 2008, Astropart. Phys., 29, 299

Burrows, D. N., et al. 2005, Space Sci. Rev., 120, 165

Cwiok, M., et al. 2008, GRB 080319b light curve by Pi-of-the-Sky, http://gcn.gsfc.nasa.gov/gcn3/7445.gcn3

Golenetskii, S., et al. 2008, Konus-Wind observation of GRB 080319B, http://gcn.gsfc.nasa.gov/gcn3/7482.gcn3

Guetta, D., Hooper, D., Alvarez-Muniz, J., Halzen, F., & Reuveni, E. 2004, Astropart. Phys., 20, 429

Hill, G. C., Hodges, J., Hughey, B., Karle, A., & Stamatikos, M. 2005, in Oxford 2005, Statistical problems in particle physics, astrophysics and cosmology, Oxford, United Kingdom, 108

Kashti, T., & Waxman, E. 2005, Phys. Rev. Lett., 95, 181101

Kumar, P., & Panaitescu, A. 2008, arXiv:0805.0144

Lundberg, J., et al. 2007, Nucl. Inst. Meth., A581, 619

Margutti, R., et al. 2008, arXiv:0809.0189

Meszaros, P., & Rees, M. J. 1993, ApJ, 405, 278

Murase, K., & Nagataki, S. 2006, Phys. Rev., D73, 0512275

NASA. 1994, Wind homepage, http://http://heasarc.gsfc.nasa.gov/docs/heasarc/missions/wind.html

Racusin, J. L., et al. 2008a, Nature, 455, 183

—. 2008b, Swift observation of GRB 080319B, http://gcn.gsfc.nasa.gov/reports/report_134_1.pdf

Razzaque, S., Meszaros, P., & Waxman, E. 2003, Phys. Rev. Lett., 90, 241103

Stamatikos, M. 2008, private communication

Stamatikos, M., (IceCube Coll.), et al. 2005, in Proc. International Cosmic Ray Conference (ICRC'05), Vol. 4, Pune, India, 471

Vreeswijk, P. M., et al. 2008, VLT/UVES redshift of GRB 080319B from FeII fine-structure lines, http://gcn.gsfc.nasa.gov/gcn3/7451.gcn3

Waxman, E., & Bahcall, J. N. 1997, Phys. Rev. Lett., 78, 2292